

## Original Article

# Evidence supporting the oncogenic role of BAZ1B in colorectal cancer

Aleksandra Grochowska<sup>1,3\*</sup>, Malgorzata Statkiewicz<sup>1\*</sup>, Maria Kulecka<sup>1,3</sup>, Magdalena Cybulska<sup>1</sup>, Zuzanna Sandowska-Markiewicz<sup>1</sup>, Michal Kopczynski<sup>1</sup>, Edyta Drezinska-Wolek<sup>2</sup>, Andrzej Tysarowski<sup>2</sup>, Monika Prochorec-Sobieszek<sup>2</sup>, Jerzy Ostrowski<sup>1,3</sup>, Michal Mikula<sup>1</sup>

Departments of <sup>1</sup>Genetics, <sup>2</sup>Pathology and Laboratory Diagnostics, Maria Sklodowska-Curie National Research Institute of Oncology, Warsaw 02-781, Poland; <sup>3</sup>Department of Gastroenterology, Hepatology and Clinical Oncology, Centre for Postgraduate Medical Education, Warsaw 01-813, Poland. \*Equal contributors.

Received July 7, 2022; Accepted September 14, 2022; Epub October 15, 2022; Published October 30, 2022

**Abstract:** Bromodomain Adjacent to Zinc Finger Domain 1B (BAZ1B) is involved in multiple nuclear processes, and its role in tumorigenesis is emerging. However, the function of BAZ1B in colorectal cancer (CRC) remains largely unexplored. High-density tissue microarrays comprising 100 pairs of matched normal colon and treatment-naïve CRC samples were analyzed by immunohistochemistry with an anti-BAZ1B antibody. The HCT116 and SW480 CRC cell lines were used for overexpression and small hairpin RNA-mediated BAZ1B knockdown models, respectively. Both cell lines were xenografted to immunodeficient NU/J mice to assess tumor burden. The molecular consequences of alterations of BAZ1B expression were assessed by RNA-Seq of xenografts and functional analyses using the Reactome database. Immunohistochemical analysis of BAZ1B showed that BAZ1B staining intensity was higher in 93 tumor specimens and significantly correlated with tumor size ( $P = 0.03$ ), but not with the presence of KRAS mutation. BAZ1B overexpression significantly increased and its knockdown inhibited the proliferation of HCT116 and SW480 cell lines, respectively. These findings were reproduced when both cell lines were grown as xenografts. RNA-Seq of HCT116 and SW480 xenografts identified 2046 and 99 differentially expressed genes (DEGs) (adjusted  $P \leq 0.05$ ), respectively. Functional annotation of DEGs identified already established as well as new molecular processes dependent on BAZ1B protein expression. In conclusion, BAZ1B is overexpressed in CRC tissue and contributes to CRC cell proliferation in vitro and in vivo. The data support the emerging oncogenic role of BAZ1B in cancerogenesis including in CRC.

**Keywords:** BAZ1B, WSTF, colorectal cancer, oncogene, xenografts, RNA-Seq

## Introduction

Epigenetic mechanisms affect phenotype by interfering with gene expression [1]. Histone acetylation is a fundamental mechanism for regulating gene transcription [2], and the acetyl marks in histone tails are read by bromodomain (BRD)-containing proteins [2]. BRDs are found in many chromatin- and transcription-associated proteins, and have various functions, including histone modification, chromatin remodeling, transcription factor recruitment, and enhancer or mediator complex assembly, and these activities affect transcription initiation and elongation [3].

Bromodomain Adjacent to Zinc Finger Domain 1B (BAZ1B), also known as Williams Syndrome Transcription Factor or WSTF, consists of sev-

eral conserved domains including a BRD that binds acetylated lysine 14 on histone H3, a plant homeodomain finger motif that interacts with the first six N-terminal residues of histone H3, and DNA interacting WAKZ and WAC domains, the latter of which has tyrosine kinase activity [4]. According to the molecular context, BAZ1B associates with ATP-dependent chromatin remodeling complexes, including the SWI/SNF ATPases Brg1 and Brm containing WINAC (WSTF including the nucleosome assembly complex), WICH (WSTF-ISWI chromatin), and the B-WICH remodeling complex [4].

BAZ1B is a modulator of chromatin remodeling complexes and thus plays many roles. BAZ1B is an important gene patterning the modern human face [5]. It is responsible for thyroid defects in Williams syndrome patients mediat-

ed by the PTEN signaling pathway [6], and it may regulate reward behaviors to distinct emotional stimuli [7]. It is essential for timely chromosome condensation at mitosis entry [8], and it catalyzes Tyr142 phosphorylation of histone H2AX (pTyr142) in somatic cells, thereby regulating the balance between DNA repair and apoptosis [9]. BAZ1B is required in T cells for mediating the effect of L-arginine on survival [10] and is involved in the transcriptional regulation of Il17a mRNA during TH17 cell differentiation [11].

We previously performed quantitative shotgun proteomics of colon healthy mucosa, adenoma, and adenocarcinoma samples, and found that the BAZ1B protein was significantly upregulated during the progression from the normal colon through adenoma to adenocarcinoma [12]. The intrinsic tyrosine kinase activity of BAZ1B may improve the sensitivity of cancer cells to radio- and chemotherapy [13]. KRAS is the most frequently mutated oncogene, with a mutation prevalence of 25% across all cancers. Approximately 40% of colorectal cancers (CRCs) carry a KRAS mutation. KRAS mutation status is associated with poorer survival, increased tumor aggressiveness, and resistance to select treatment strategies [14]. In colon cancer cells, mutation of KRAS glycine 12 to valine (G12V) induces the “secretion” of intracellular non-secretory BAZ1B by activating the silenced secretory protein-neuregulin-3 (NRG3), leading to the activation of oncogenic pathways in the surrounding normal colon cells and promoting the formation of colon tumors [15].

In this study, we show that BAZ1B is upregulated in CRC in correlation with tumor size. BAZ1B overexpression increased, whereas its transient knockdown inhibited the proliferation of CRC cells *in vitro* and *in vivo* in a xenograft tumor model. Functional annotation of differentially expressed transcripts in xenograft models identified already established and new molecular processes associated with BAZ1B protein expression. Overall, the present data support the oncogenic role of BAZ1B in CRC progression.

### Materials and methods

#### Patients

A group of a hundred patients with CRC diagnosed according to WHO criteria [16], and treat-

ed in Maria Sklodowska-Curie National Research Institute of Oncology were enrolled in this study, with a male to female ratio 59:41 and median age 64.2 years old (range: 36-85, SD = 11). Tumors size was evaluated during the macroscopic examination of the fixed tissue material. The largest linear dimension of the tumor in cm was considered. The mean size of the tumor was 4.3 cm (range: 1.7-9.0 cm, SD = 1.8). Most of the patients were defined as pT3 (70%) and pN0 (63%) according to TNM staging system (Table S1). The informed consent was obtained from all patients. The experiments conformed to the principles set out in the WMA Declaration of Helsinki and the Department of Health and Human Services Belmont Report. The study protocol for archival patients' samples was approved by the Bioethics Committee of the Maria Sklodowska-Curie National Research Institute of Oncology in Warsaw (decision No. 40/2017).

#### Cell culture

All cell lines were purchased from American Type Culture Collection. Colo205 and SW480 were grown in RPMI (#10432512; Thermo Fisher Scientific, Waltham, MA, USA) supplemented with heat-inactivated 10% FBS (#F7524; Sigma-Aldrich, Saint Louis, MO, USA); HT29 and HCT116 cells were grown in McCoy (M9309; Sigma-Aldrich, Saint Louis, MO, USA) supplemented with heat-inactivated 10% FBS. The media were also supplemented with penicillin (100 I.U./ml) and streptomycin (100 µg/ml) (Sigma-Aldrich, Saint Louis, MO, USA) and 2 mmol/l L-glutamine (Sigma-Aldrich, Saint Louis, MO, USA). Cells were cultured at 37°C with 10% CO<sub>2</sub>. Medium changes and cells passages were performed every 3-4 days.

#### RNA extraction and cDNA synthesis

Total RNA was extracted from frozen cells and tumors using Direct-zol MiniPrep Kit (Cat# R2052; Zymo Research, Irvine, CA, USA), and complementary DNA (cDNA) was transcribed from mRNA using SuperScript VILO cDNA Synthesis Kit (Cat# 11754050; Thermo Fisher Scientific, Waltham, MA, USA), according to the manufacturer's protocols. Briefly, cell pellets were lysed up while tumor tissue homogenized using a homogenizer in TRI reagent, then ethanol was added and a sample was transferred into a column. DNAase treatment was performed and a column was washed. RNA was

## Oncogenic role of BAZ1B in colorectal cancer

eluted in water by centrifugation. RNA quantity, purity, and quality were determined using *NanoDrom* (Thermo Fisher Scientific, Waltham, MA, USA) and Qubit Fluorometer (Thermo Fisher Scientific, Waltham, MA, USA). 500 µg of total RNA was used for cDNA reaction. The resulting cDNA was 5-fold diluted in water for PCR reaction.

### *Reverse-transcriptase (RT) quantitative (Q) PCR*

BAZ1B mRNA expression was quantified by RT-qPCR using TaqMan assay (Hs002248-31-m1; Thermo Fisher Scientific, Waltham, MA, USA) and normalized to a reference RPLPO transcript (Hs00420895-gH; Thermo Fisher Scientific, Waltham, MA, USA). PCR reactions were performed in triplicates on Applied Biosystems 7900HT Fast Real-Time PCR System as described before [12]. RT-qPCR data were normalized to the expression of RPLPO mRNAs using the  $\Delta\Delta C_t$  method where delta Ct was the difference in the BAZ1B Ct values and the endogenous RPLPO control [17]. The delta-delta value was calculated as the difference between the delta Ct of the treated sample and to control sample. This value was used to calculate fold change. No template controls (NTCs) were performed to detect the presence of contaminating DNA.

### *Western blot*

Cells were lysed in the RIPA buffer containing 150 mM NaCl, 1% NP40, 0.5% deoxycholic acid, 0.1% SDS, 50 mM Tris (pH 8.0) and homogenized using Bioruptor (Diagenode). Protein concentrations of the lysates were determined by the Pierce BCA Protein Assay Kit (Thermo Fisher Scientific, Waltham, MA, USA). Lysates (20 µg of protein per well) were resolved in 10% SDS-PAGE gels and subsequently transferred to Immobilon PVDF membranes (Merck Millipore, Burlington, MA, USA). The blots were probed with the anti-human BAZ1B rabbit primary antibodies (W3641; Sigma-Aldrich, Saint Louis, MO, USA), followed by Goat Anti-Rabbit IgG (H+L) HRP-conjugated secondary antibodies (172-1019; BioRad, Hercules, CA, USA). Primary and secondary antibodies were used in dilution ratio of 1:5000 and 1:10000, respectively. Signals from reactive bands were visualized by a chemiluminescence detection system (CPS530-1KT; Sigma-Aldrich, Saint Louis, MO, USA) and documented using UVITEC mini HD4 (Uvitec, Cambridge, UK).

### *Proliferation assay*

Cells were seeded in 96-well plates at a density of  $2 \times 10^3$  cells/well. Cell viability and proliferation were measured by the crystal violet assay. The attached live cells were stained with 0.5% crystal violet solution in 25% methanol every day. After washing out the dye, cells were dried at room temperatures. On the same day, when all the plates have already been stained and dried, the bound dye was dissolved in 33% acetic acid solution and the absorbance of solutions was read spectrophotometrically at 540 nm.

### *Colony formation assay*

Cells were seeded in 6-well plates and incubated for 14 days (transient transfected HCT116 and SW480 cells) or 5 days (stably transfected SW480 shBAZ1B, HCT116 Ctrl and HCT116 BAZ1B cells) in the number of  $10^4$  (transient transfection),  $10^5$  (stable transfected HCT116 Ctrl and HCT116 BAZ1B) and  $2 \times 10^5$  (stable transfected SW480 BAZ1B). Then, crystal violet staining was performed and the number of colonies consisting of 50 or more cells was manually counted.

### *Transient transfection with small interfering RNA (siRNA)*

Cells were transfected with siRNA (at a final concentration of 30 nM), which targeted exomes 8 and 9 of BAZ1B (s17208; Thermo Fisher Scientific, Waltham, MA, USA) using Lipofectamine RNAiMAX (Thermo Fisher Scientific, Waltham, MA, USA), in Opti-MEM medium (Thermo Fisher Scientific, Waltham, MA, USA), according to manufacturer's recommendations. Scrambled siRNA (4390844; Thermo Fisher Scientific, Waltham, MA, USA) was used as the negative control. The experiments were conducted in technical triplicates and at least in three biological replicates. Before further processing cells were silenced for 48 hrs unless otherwise indicated. Each time BAZ1B knockdown was verified by RT-qPCR and western blot.

### *Construction and establishment of stably transfected cell lines*

To generate stable BAZ1B overexpression cells, HCT116 cells were transfected with the pcDNA6.2/N-EmGFP-DEST plasmid containing

## Oncogenic role of BAZ1B in colorectal cancer

the insert from the coding sequences of the BAZ1B gene under the constitutive CMV promoter (obtained from Addgene; Plasmid #65372 [18]). Single-cell clones were isolated by a 7 µg/ml blasticidin-containing medium. Empty vector-infected cells were used as control. Overexpression of BAZ1B was confirmed by western blot.

To generate stable BAZ1B knockdown cells, SW480 cells were two-staged transfected by the two plasmid constructs. Firstly, the cells were transfected with pcDNA6/TR plasmid to obtain a line with stable expression of the TetR protein, allowing induction of shRNA expression silencing the BAZ1B gene; the TetR protein sequence is encoded under the constitutive CMV promoter. Single-cell clones were isolated by a 7 µg/ml blasticidin-containing medium. Cells with a stable expression of the TetR protein were then transfected with plasmid pEN-TRTM/H1/TO to establish a stable induced silencing system; the coding sequence for shRNA molecules (shRNA fwd 5'-CACCGC-ACAGATCGAAACCATAATACGAATATTATGGT-TTCGATCTCTGC-3'; shRNA rev 3'-CGTGTCTAGCTTTGGTATTATGCTTATAATACCAAAGCTAG-AGACGAAAA-5') has been encoded under the H1/TO promoter having TetR protein attachment sites. Single-cell clones were isolated by 150 µg/ml Zeocin-containing medium. Silencing induction was carried out by 2 µg/ml doxycycline stimulation.

### *Xenograft experiments*

NU/J (nude) athymic mice were purchased from The Jackson Laboratory and maintained in a specific pathogen-free (SPF) facility. The breeding strategy was performed as described before [19]. To establish a cell line xenografts,  $5 \times 10^6$  cells of parental or transformed SW480 and HCT116 cell lines were injected subcutaneously into a flank of 40 and 20, respectively, 6-8 weeks old male mice [20]. Of 40 mice grafted with SW480 cells, 20 mice were injected with cells encoding an induced BAZ1B silencing system, and the other 20 mice with cells with the construct encoding the TetR protein (control variant). When tumors reached on an average volume of 100 mm<sup>3</sup>, the animals were divided into four groups (n = 10), of which two received doxycycline in drinking water. HCT116 cells with control empty plasmid or BAZ1B-

overexpressing HCT116 cells were grafted subcutaneously to the nude mice and tumors measurements started when reached on an average volume of 100 mm<sup>3</sup>. Tumor volume was measured and calculated automatically by the software coupled with a Peira TM900 (Peira bvba, Beerse, BE) handheld device. All animal work was performed under a protocol approved by the Local Ethics Committee (decision WAW2/095/2018 and WAW2/096/2018 for HCT116 and SW480 cell lines, respectively).

### *Immunohistochemistry staining of CRC patients' tumors*

High-density tissue microarrays were made from formalin-fixed paraffin-embedded (FFPE) samples of a hundred matched pairs of treatment-naïve CRC samples and normal colon. The staining was conducted using an automated immunohistochemical stainer (Dako Denmark A/S) with anti-BAZ1B antibodies (W3641; Sigma-Aldrich, Saint Louis, MO, USA). The EnVision Detection System (Agilent Technologies, Santa Clara, CA, USA) was used for detection. Samples were reviewed for an abundance of BAZ1B protein in normal and cancerous tissues by two pathologists. A semi-quantitative method involving a scoring system was used to assess IHC staining, intensity: 0-no staining; 1-weak, 2-intermediate, and 3-strong staining; staining homogeneity was above 90%.

### *KRAS mutations status determination*

DNA from a 5 µm thick FFPE section was extracted with the use of QIAamp® DNA Mini-Kit (#51304; Qiagen, Hilden, Germany). The KRAS mutations were surveyed with AmoyDx KRAS Mutation Detection Kit (Amoy Diagnostic, Xiamen, Fujian, China) on 7900HT Fast Real-Time PCR System (Applied Biosystems, Foster City, CA, USA) according to the manufacturer recommendations. The AmoyDx kit provides the DNA samples with KRAS mutations and these samples were included as a positive control during each run.

### *Transcriptome analysis*

Total RNA concentration was measured using a Qubit instrument and Qubit RNA HS Assay Kit (Thermo Fisher Scientific, Waltham, MA, USA), according to the manufacturer's protocol. Total

RNA quality and integrity were assessed using Agilent RNA kits on a Bioanalyzer 2100 (Agilent Technologies, Santa Clara, CA, USA). The samples were submitted to the Fasteris Service (Plan-les-Ouates, Switzerland) where library preparation was conducted and sequenced on an Ion Proton sequencer. The sequencing data were provided as raw BAM files. Transcripts were quantified using HTseq-count (version 0.6.0) [21], run with default options. Differential gene expression was evaluated with DESeq2 [22]. Before comparisons were made, the 20% of genes with the lowest normalized read counts across all samples were removed. The clusterProfiler package was used the Reactome pathway for functional analyses [23]. All calculations were performed in the R environment. The results were corrected for multiple testing according to the Benjamini and Hochberg procedure with the threshold of statistical significance of  $P < 0.05$ .

### Results

#### *BAZ1B abundance is increased in CRC tissue and correlates with tumor size*

In previous work, we used a shotgun proteomics approach and showed that the BAZ1B protein is overexpressed in CRC [12]. To confirm this observation and examine BAZ1B expression in other malignancies, we screened The Cancer Genome Atlas (TCGA) using the Gepia webserver browser [24] by comparing its expression between different tumors and matching healthy tissues. The results showed that BAZ1B mRNA is significantly overexpressed in several cancers, including colon and rectum adenocarcinomas, cholangiocarcinoma, esophageal carcinoma, head and neck squamous cell carcinoma, liver hepatocellular carcinoma, gastric adenocarcinoma, and sarcoma (**Figure 1A**). Because gene expression alterations can be caused by genetic aberrations related to somatic copy-number alterations (SCNAs) [25], we explored this possibility for BAZ1B using the TCGA pan-cancer dataset. Narrowing down the list of samples to a set of samples with both BAZ1B mRNA expression and SCNA datasets yielded 10,035 TCGA pan-cancer samples, of which 380 were CRC. The collation of both datasets showed that BAZ1B mRNA was correlated with SCNA, with a Spearman correlation of 0.42 and 0.47 for the

pan-cancer and CRC samples, respectively (**Figure 1B**). To determine whether the mRNA abundance was associated with increased BAZ1B protein abundance in CRC, we performed BAZ1B immunohistochemistry (IHC) staining on tissue microarrays covering 100 pairs of matched human normal colon and treatment-naïve primary CRC samples (**Table S1**). Semi-quantitative staining of the BAZ1B protein was performed using the following scoring system based on intensity: 0, no staining; 1, weak; 2, intermediate; and 3, strong staining. The results showed increased nuclear staining intensity in 93 CRC specimens compared with the corresponding normal colon mucosa; in 28 of these specimens, BAZ1B protein levels were at least two intensity units higher in tumor samples (**Figure 1C**). Analysis of accompanying clinical and genetic data showed a significant correlation between BAZ1B staining intensity and tumor size ( $P = 0.03$ ) (**Figure S1**). Because a previous study suggested a link between the KRAS G12 mutation and BAZ1B expression [15], we collated the genetic data for KRAS status as a diagnostic procedure. The genetic data were available for 63 CRC tissues, of which 18 (28%) were KRAS mutation-positive. However, neither KRAS mutations tested as a whole nor as separate variants (G12/G13/Q61) correlated with the BAZ1B staining score. The analysis of TCGA dataset confirmed that BAZ1B mRNA is overexpressed in various malignancies including CRC and revealed a significant correlation between BAZ1B mRNA expression and SCNA in CRC. Increased BAZ1B mRNA levels in CRC were correlated with increased, predominantly nuclear, protein abundance and with tumor size.

#### *Alterations of BAZ1B protein expression affect the clonogenicity and proliferation of CRC cells*

To select cell lines for functional experiments, we first estimated the relative BAZ1B expression in five CRC cell lines, including Colo205, RKO, HT29, HCT116, and SW480, using RT-qPCR and western blotting. BAZ1B transcript levels were highest in SW480 cells and lowest in RKO cells, whereas BAZ1B protein expression was highest in SW480 cells and lowest in Colo205 cells (**Figure 2A**). Of the five cell lines tested, the HCT116 and SW480 cell lines have mutated KRAS at G13D and G12V [26], respectively, and the link between consti-

# Oncogenic role of BAZ1B in colorectal cancer

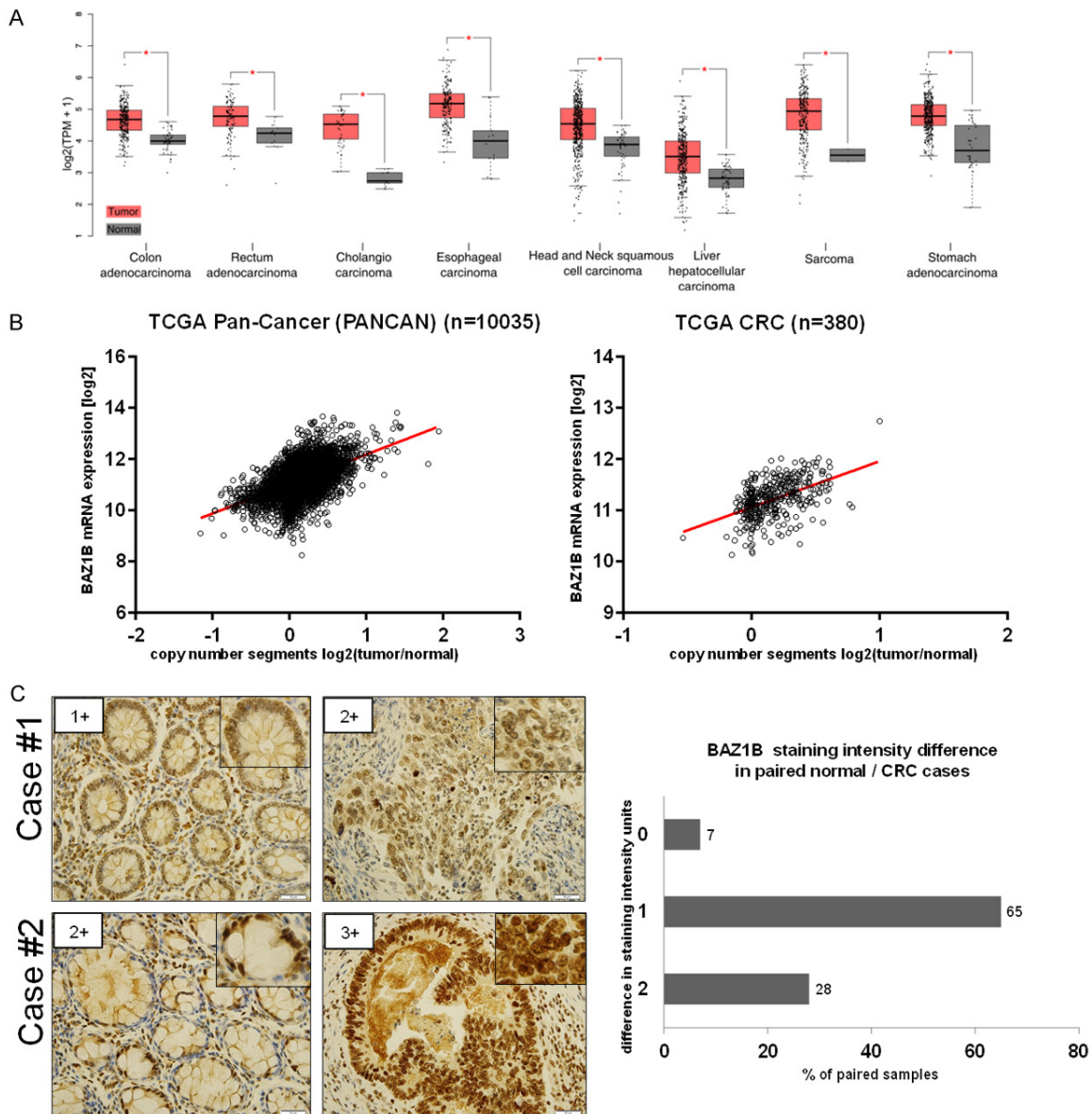
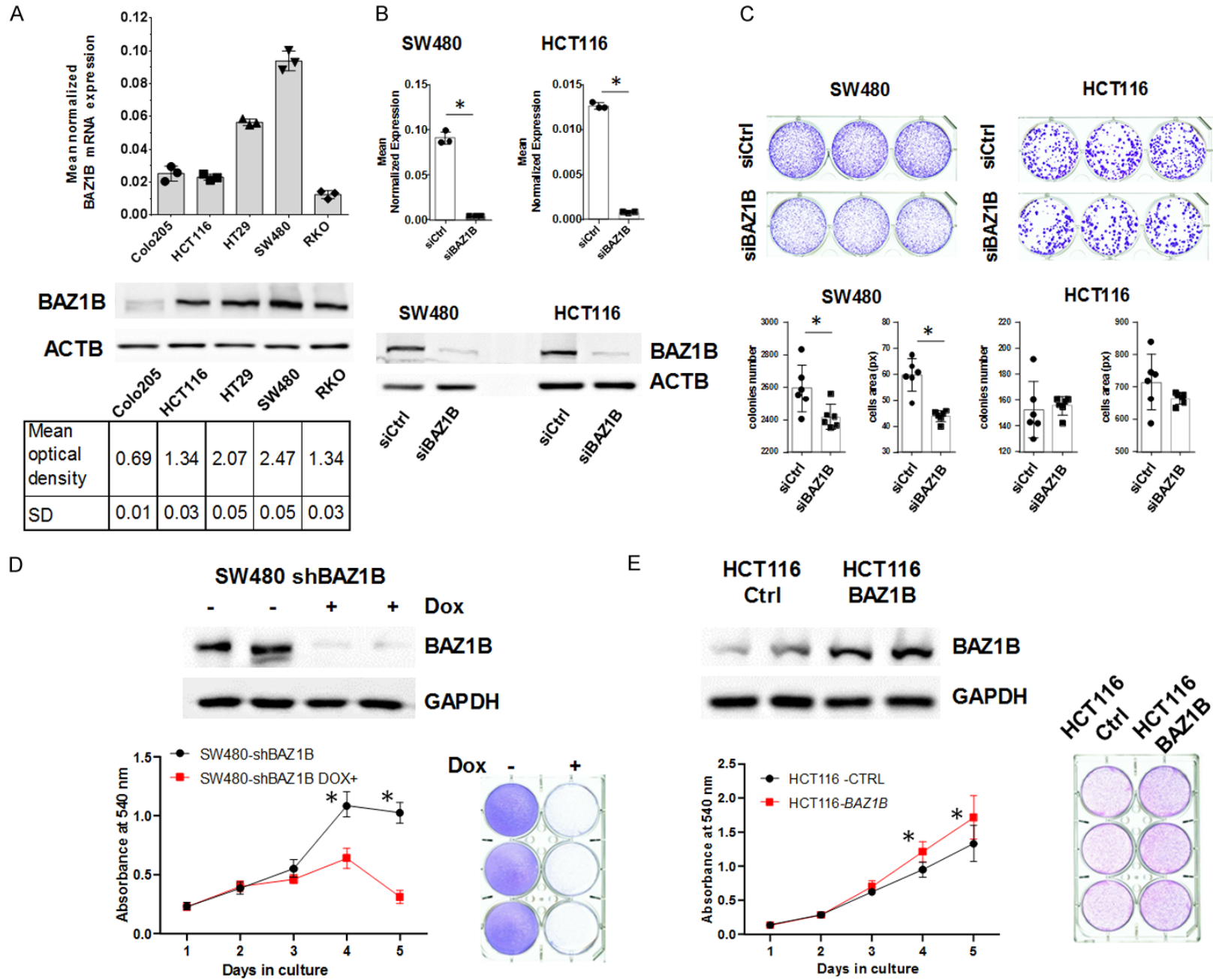


**Figure 1.** BAZ1B abundance is increased in CRC tissue and correlates with tumor size. A. The BAZ1B mRNA is increased in multiple malignancies including colorectal cancer. The Cancer Genome Atlas (TCGA) pan-cancer gene expression profiles of BAZ1B were analyzed using the Gene Expression Profiling Interactive Analysis (GEPIA2) database at a fold change of 1.5 and a p of 0.05 cutoff (\*). B. Correlation of BAZ1B mRNA abundance with somatic copy-number alterations (SCNAs) in TCGA Pan-Cancer and CRC dataset. mRNA and SCNA data were obtained using the UCSC Xena browser [42]. Tumor SCNAs are presented after removing germline values. C. Immunohistochemical (IHC) evaluation of BAZ1B confirms its overexpression in colorectal cancer. Left panel. IHC staining of BAZ1B in normal colon and matched colon cancer samples as an example of the staining scoring system: 3+-very intensive staining, 2+-medium-intensive staining, 1+-weak staining. Scale bar, 20  $\mu$ m. Case#1: normal colon mucosa with weak nuclear staining, colon cancer with moderate (2+) nuclear staining intensity, case#2: (left) normal colon mucosa with nuclear moderate staining (2+), (right) colon cancer with strong nuclear staining (3+); (all photographs: 400x). Scale bar, 20  $\mu$ m. Inserts were included to highlight BAZ1B nuclear localization. Right panel. Analysis of BAZ1B IHC staining performed on 100 pairs of normal colon and matched colon cancer samples shows its nuclear localization and confirms its overexpression in tumor tissue. Source data are available in [Table S1](#).

tutively active KRAS status and BAZ1B expression was shown previously [15]. We therefore selected the two cells lines for further experiments. To investigate the effect of BAZ1B

depletion on the growth and proliferative characteristics of the two cell lines, we first confirmed the efficient BAZ1B knockdown at the mRNA and protein levels in both cell lines

Oncogenic role of BAZ1B in colorectal cancer



## Oncogenic role of BAZ1B in colorectal cancer

**Figure 2.** Alternation of BAZ1B protein expression influences clonogenicity and proliferation of CRC cell lines. (A) BAZ1B transcript (upper panel) and protein abundance (lower panel) in the panel of CRC cell lines. RT-qPCR data represent normalized mean BAZ1B transcript expression  $\pm$  SD measured in three independent experiments. Western blotting was performed on cell lysates stained with the anti-BAZ1B and beta-Actin (ACTB) antibodies. ACTB was used as a loading control. The images show the representative results of two independent protein isolations. The intensities of BAZ1B were normalized to ACTB bands. Bands were analyzed densitometrically with OptiQuant (B). MRNA levels (upper panel) and protein (lower panel) of BAZ1B abundance in SW480 and HCT116 cells 48 hours following transfection with non-targeting (siCtrl) and BAZ1B-targeting (siBAZ1B) siRNAs. MRNA and protein isolation and analysis were performed as in (A). The presented graphs show the average values  $\pm$  SD from three independent experiments. Error bars are SD. Two-tailed unpaired t-test; \* $P \leq 0.0001$ . (C) Analysis of clonogenic growth of SW480 and HCT116 cells assessed 14 days after transfection with siCTRL and siBAZ1B. The presented graphs show the average values  $\pm$  SD from three independent experiments. Error bars are SD. Two-tailed unpaired t-test; \* $P \leq 0.05$ . (D) SW480 cells expressing a BAZ1B shRNA were treated with 2  $\mu$ g/ml doxycycline (Dox) for 72 hours and tested for BAZ1B knockdown with Western blot as in (A). GAPDH antibody was used as a loading control. For proliferation assay,  $2 \times 10^3$  SW480 cells were seeded and stained with crystal violet at the indicated time points and then dissolved for spectrophotometric reading. Each assay condition was done with at least 16 technical replicates. Values are means of four independent experiments. Error bars are SD. Two-way ANOVA; \* $P \leq 0.05$ . A representative crystal violet stained 6-well plate with SW480 BAZ1B shRNA cell with and without Dox treatment on the 5<sup>th</sup> day is shown. (E) HCT116 cells either transfected with the empty pcDNA6.2/N-EmGFP-DEST plasmid or the same plasmid containing BAZ1B gene were cultured for 72 hours at assayed with Western blot as in (D). For proliferation assay  $2 \times 10^3$  HCT116 cells of each type were seeded and stained with crystal violet at the indicated time points and then dissolved for spectrophotometric reading. Representative crystal violet stained 6-well plate from the 5<sup>th</sup> day is shown. The number of independent experiments and statistical analyses used is the same as in (D).

(**Figure 2B**), and then performed clonogenic assays after siRNA-mediated BAZ1B transient silencing. The results of the clonogenic assay showed that BAZ1B depletion significantly decreased colony formation and the mean area of colonies in SW480 cells but not in HCT116 cells (**Figure 2C**). Next, the SW480 line was used to generate a doxycycline-induced BAZ1B silencing model in which the stable clone showed 90% silencing after cell treatment with doxycycline (**Figure S2A**). The HCT116 cell line was used to generate a stable BAZ1B overexpression model. BAZ1B expression was 5-fold higher in the HCT116 clone transfected with a BAZ1B-expressing plasmid than in wild-type cells and higher than in the SW480 line, whereas BAZ1B expression in the control clone transfected with an empty plasmid was comparable with that in wild-type HCT116 cells (**Figure S2B**). Cell proliferation was significantly lower in SW480 cells with doxycycline-induced expression of anti-BAZ1B shRNA than in empty plasmid-transfected control cells (**Figure 2D**), whereas HCT116 cells with stable BAZ1B overexpression exhibited a higher proliferation rate than control cells (**Figure 2E**). Collectively, the *in vitro* results indicate that BAZ1B abundance affects the proliferation rate of CRC cells.

*BAZ1B depletion inhibits, whereas overexpression stimulates, the growth of CRC cell lines in vivo*

To evaluate the effects of BAZ1B expression on CRC *in vivo*, we compared the ability of both cell

lines to give rise to subcutaneous tumors in nude mice. Of 40 nude mice grafted with SW480 cells, 20 were injected with cells encoding an induced BAZ1B silencing system and the other 20 mice received cells containing the construct encoding the TetR protein (control variant). When tumors reached an average volume of 100 mm<sup>3</sup>, the animals were divided into two groups, of which one received doxycycline in drinking water to induce shRNA expression in tumor cells. Mice bearing SW480 tumors expressing the TetR protein with and without doxycycline exhibited the same rate of growth (**Figure S3**). Doxycycline-induced shRNA-BAZ1B expression in SW480 cells delayed xenograft tumor growth, and the difference reached statistical significance at the end of the experiment on the 22<sup>nd</sup> day of doxycycline administration (**Figure 3A**).

Ten nude mice were grafted subcutaneously with control empty plasmid HCT116 cells or BAZ1B-overexpressing HCT116 cells. The tumor growth rate was significantly higher in xenografts overexpressing BAZ1B than in controls (**Figure 3B**). At the end of the experiment, portions of each xenograft were cryopreserved for western blotting and transcriptomic assays. Western blot analysis of protein lysates from xenografts confirmed the depletion and increase in BAZ1B protein abundance in SW480 BAZ1B shRNA and HCT116 BAZ1B tumors, respectively (**Figure 3C, 3D**). Taken together, *in vivo* experiments confirmed that manipulation of BAZ1B expression in CRC cell

## Oncogenic role of BAZ1B in colorectal cancer

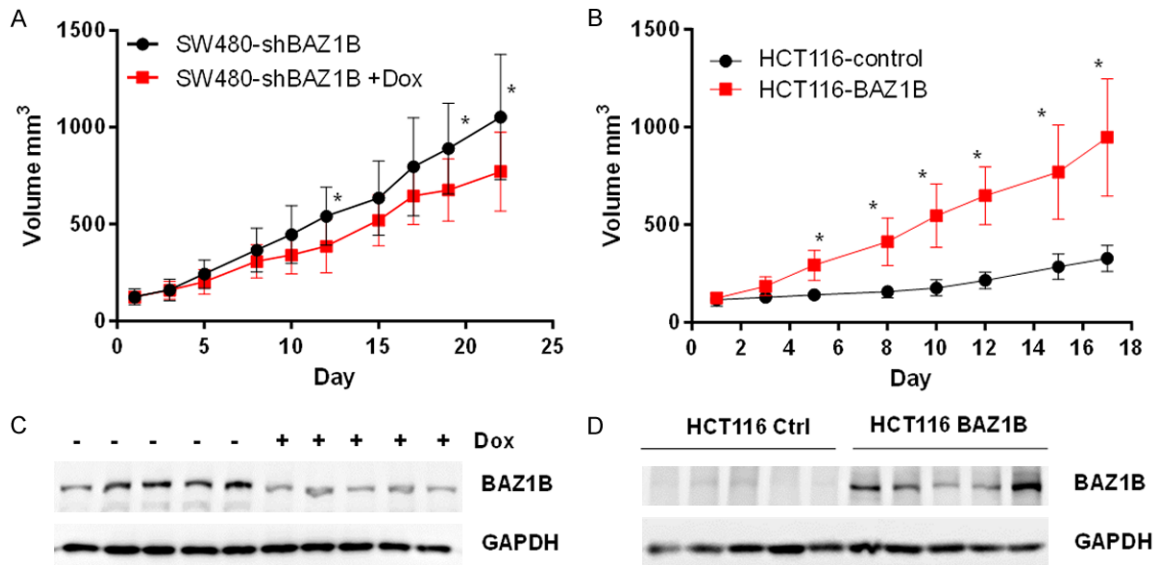


**Figure 3.** BAZ1B depletion inhibits while overexpression stimulates the growth of CRC cells in vivo. A. Tumor volumes of subcutaneous SW480 shRNA-BAZ1B xenografts following 22 days of doxycycline administration. Doxycycline administration and measurements were initiated when tumors reached an average size of 100 mm<sup>3</sup>, n = 9 for each group, each mouse bearing one tumor,  $\pm$  SD. Two-way ANOVA; \*P  $\leq$  0.05. B. Tumor volumes of subcutaneously grown HCT116 control (transfected with empty plasmid) and BAZ1B overexpressing HCT116 cells following 17 days of observation. Tumor volume measurements started when tumors reached an average size of 100 mm<sup>3</sup>, n = 10 for each group, each mouse bearing one tumor,  $\pm$  SD. Two-way ANOVA; \*P  $\leq$  0.05. C. and D. Western blot analysis of protein lysates from SW480 and HCT116 xenografts confirms BAZ1B alternation in those tumors. The amount of 20  $\mu$ g of protein lysate was resolved with SDS-PAGE, electrotransferred to PVDF membrane, and immunoblotted with the anti-BAZ1B and anti-GAPDH antibodies. GAPDH was used as a loading control.

lines affects their potential to grow as xenografts.

### *BAZ1B expression changes affect similar molecular pathways in CRC xenografts*

To identify the molecular pathways affected by changes in BAZ1B expression, we performed a transcriptomic survey of tumors collected from the xenograft experiment. In total, 24 poly (A)-enriched mRNA samples isolated from six xenograft tissue samples of SW480 shRNA-BAZ1B with and without doxycycline, as well as HCT116 control and BAZ1B-overexpressing cells, were subjected to RNA-Seq analysis. Principal component analysis (PCA) differentiated HCT116 control xenograft tumors from those with stable BAZ1B overexpression and, to a lesser degree, xenografts from the SW480 shRNA-BAZ1B cell line with and without doxycycline treatment (Figure S4). Pairwise comparisons between HCT116 control and BAZ1B-overexpressing xenografts identified 2046 differentially expressed genes (DEGs) (1019 downregulated and 1027 upregulated) (adjusted P < 0.05) (Table S2), and 99 DEGs (36 down-

regulated and 63 upregulated) were identified in the comparison of SW480 shRNA-BAZ1B +/- Dox xenografts (Table S3; Figure 4A). Nine genes (GNAI1, ITGA10, RPL34, LTA4H, SLC2A3, RPS4X, CDK6, COL17A1, and TOMM7) were common and showed the opposite direction of expression in both comparisons. To identify molecular alterations related to changes in BAZ1B abundance, we performed functional analyses of significantly up- and downregulated DEGs (adjusted P < 0.05) using the Reactome database. The functional analysis yielded 1/216 and 33/0 significantly enriched pathways for up/downregulated DEGs in HCT116 and SW480 xenografts, respectively (Table S4). In the BAZ1B overexpressing HCT116 cell line, the downregulated genes were over-represented in 48 pathways belonging to the Cell Cycle Reactome master term. The Cell Cycle term comprised a set of 70 downregulated genes. Some of these genes, including CDKN1A (FC = 0.48) and MDM2 (FC = 0.64), were described previously as master negative regulators of cell proliferation [27, 28]. Additionally, the set contained 14 downregulated genes encoding con-

## Oncogenic role of BAZ1B in colorectal cancer

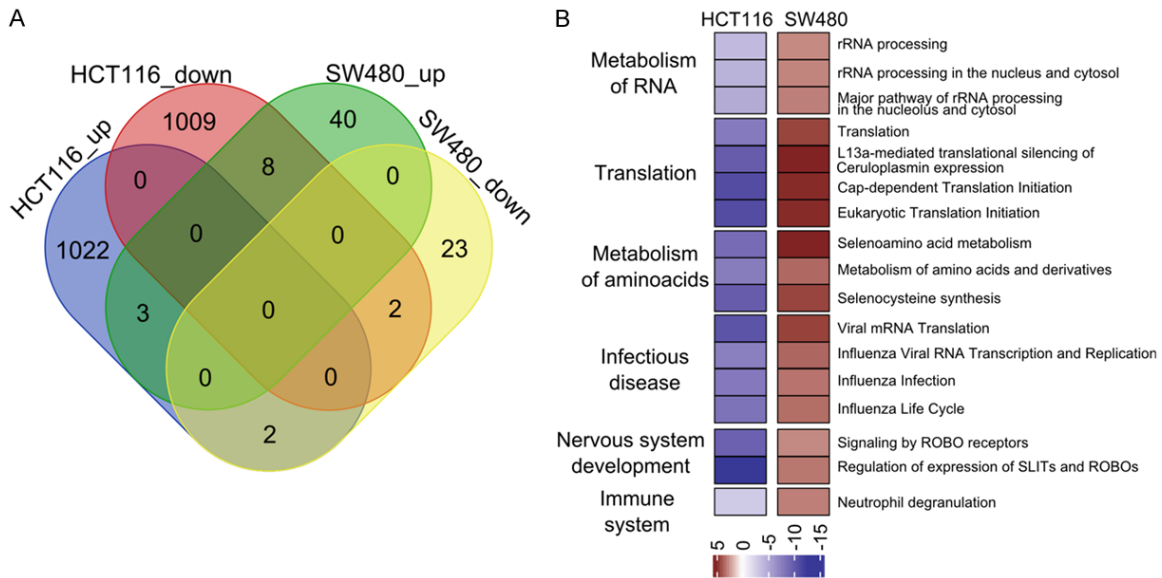


**Figure 4.** BAZ1B expression alternation influences similar molecular pathways in CRC xenografts. **A.** Venn diagram showing the number of upregulated (up) and downregulated (down) DEGs (an adjusted  $P < 0.05$ ) within HCT116 and SW480 cells line models pair-wise comparisons. The diagram was created with an online tool <http://bioinformatics.psb.ugent.be/webtools/Venn/>. **B.** Significantly altered (adj.  $P < 0.05$ ) common Reactome terms for HCT116 and SW480 cells line models pair-wise comparisons. The Reactome pathways with a differential gene ratio higher than 10% are shown. The p is shown on the PHRED scale and is reversed for downregulated pathways. The heatmap of common pathways was prepared with the clusterProfiler package.

stituents of the proteasome complex (PSMA3, PSMA5, PSMB1, PSMB7, PSMC2, PSMD1, PSMD11, PSMD12, PSMD14, PSMD2, PSMD6, PSMD7, PSME3, and PSME4). Of those, PSME3 and PSME4, which encode the PA28 $\gamma$  and PA200 proteins, respectively, are located in the nucleus and are essential regulators of proteasome activity towards chromatin-associated and cell cycle proteins [29, 30]. Thirty pathways were common to downregulated DEGs in HCT116 xenografts and upregulated DEGs in SW480 xenografts; of these, 17 pathways included at least 10% of changed DEGs in a given comparison (**Figure 4B**). Consistent with the role of BAZ1B in ATP-dependent chromatin remodeling protein complexes [31], most of the pathway terms were related to the metabolism of rRNA and proteins as well as nervous system development pathways. In addition, the analysis revealed associations of BAZ1B with pathways related to infectious diseases and the immune system. In conclusion, the transcriptomic survey for both xenograft models revealed common molecular alterations that were functionally connected to already established and possible new cellular roles of the BAZ1B protein.

## Discussion

In this study, immunohistochemistry staining using a Human Protein Atlas-validated antibody [32] showed that BAZ1B was upregulated in colon adenocarcinoma tissue samples compared with the corresponding normal mucosa, and BAZ1B staining intensity was positively correlated with increased tumor size. The correlation of BAZ1B abundance in tumor tissue with KRAS mutation status was not confirmed, although such an association was previously demonstrated for serum BAZ1B in CRC patients with a KRAS mutation at G12 [15]. Overexpression of BAZ1B increased cell proliferation, whereas BAZ1B knockdown had the opposite effect in both *in vitro* and *in vivo* cancer models, suggesting that BAZ1B is involved in CRC progression and thus exhibits oncogenic properties. Functional experiments support the oncogenic role of BAZ1B in lung cancer [33]; its overexpression promotes lung cancer cell proliferation and invasion *in vitro* and xenograft tumor growth *in vivo*. BAZ1B overexpression in lung cancer models induces epithelial-mesenchymal transition (EMT) through the PI3K/Akt and IL-6/STAT3 signaling pathways [33]. The

association of BAZ1B with EMT was confirmed in a recent study. BAZ1B lysine 426 acetylation by the acetyltransferase MOF increases the kinase and transcriptional regulatory activity of BAZ1B, and acetylation promotes cancer cell proliferation, invasion, EMT-related gene expression, and tumor formation, which are factors significantly correlated with breast tumor size and histological grade [34]. These observations indicate that BAZ1B acetylation by MOF is a cancer-promoting factor in breast cancer. The upregulation of BAZ1B in tumors and its oncogenic role were reported in glioblastoma [35] and cervical cancer [36]. In these malignancies, BAZ1B overexpression in cellular models increases cell proliferation and invasion concomitant with the activation of the PI3K/AKT pathway. Functional analyses of transcriptomic data identified common cellular processes associated with changes in BAZ1B expression in the two xenograft models; these processes, which are involved in BAZ1B function, include rRNA transcription [37] and protein metabolism [31], as well as nervous system development [38]. Additionally, new cellular pathways associated with BAZ1B were identified, including processes related to infectious diseases and the immune system. Functional analysis of DEGs in BAZ1B-overexpressing HCT116 tumors showed that several cell cycle-related genes were among the downregulated genes. This finding, which is inconsistent with the observed increase in cell proliferation in BAZ1B-overexpressing HCT116 tumors, could be attributed to the downregulation of important cell cycle inhibitors including CDKN1A and MDM2. CDKN1A, which is known as p21, arrests cell cycle progression by inhibiting the activity of cyclin-dependent kinases [27]. MDM2 functions as an E3 ubiquitin ligase and is a key regulator of the p53 tumor suppressor protein [39]; its depletion promotes tumorigenesis [28]. The set of downregulated genes included many transcripts encoding components of the proteasome. Among them, the proteasome regulatory units PA28 $\gamma$  and PA200 mediate the proteasomal activity of the complex and protein turnover in the nucleus [29, 30]. Additional functional studies are necessary to examine the molecular changes associated with BAZ1B overexpression and to confirm their causative relationship with tumor growth.

Readers of histone post-translational modifications including BAZ1B, which act within multi-

domain protein complexes, are structurally diverse proteins that contain one or more conserved and highly specialized domains. Of these, BRD proteins may act as transcription co-regulators, transcriptional repressors, histone acetyltransferases, E3 ubiquitin ligases, and chromatin remodelers [3]. Druggability is an important concept in the process of discovery and development of new chemical entities, and is mostly restricted to small molecules [40]. To determine the degree of druggability using a small molecule approach, it is necessary to know the crystal structure of the analyzed protein. Although the BRD structures of the proteins encoded by BAZ2A and BAZ2B have been resolved and specific inhibitors have been developed [41], the crystal structure of the BAZ1B BRD or kinase domain has not been elucidated, preventing *in silico* predictions of druggability. The identification of new therapeutic targets is a prerequisite for cancer drug development. In this study, in addition to confirming the involvement of BAZ1B in cervical cancer [36], lung cancer [33], breast cancer [34], and glioblastoma [35], we showed that BAZ1B is upregulated in CRC tumor specimens, and modulation of BAZ1B expression affects the proliferation of CRC models *in vitro* and *in vivo*. We believe that the collected evidence is substantial enough to designate BAZ1B as an oncogene and as a feasible target for future drug development. However, further research is warranted to identify BAZ1B domains that could serve as targets for anti-cancer therapies before initiating a drug development campaign.

### Acknowledgements

The study was funded by the National Centre for Research and Development (STRATEGMED1/233574/15/NCBR/2015, EPITHERON, to J.O.).

### Disclosure of conflict of interest

None.

**Address correspondence to:** Drs. Michal Mikula and Jerzy Ostrowski, Department of Genetics, Maria Skłodowska-Curie National Research Institute of Oncology, Warsaw 02-781, Poland. Tel: +48-22-546-26-55; E-mail: michal.mikula@pib-nio.pl (MM); Tel: +48-22-546-25-75; E-mail: jostrow@warman.com.pl (JO)

## Oncogenic role of BAZ1B in colorectal cancer

### References

- [1] Kagohara LT, Stein-O'Brien GL, Kelley D, Flam E, Wick HC, Danilova LV, Easwaran H, Favorov AV, Qian J, Gaykalova DA and Fertig EJ. Epigenetic regulation of gene expression in cancer: techniques, resources and analysis. *Brief Funct Genomics* 2018; 17: 49-63.
- [2] Haynes SR, Dollard C, Winston F, Beck S, Trowsdale J and Dawid IB. The bromodomain: a conserved sequence found in human, *Drosophila* and yeast proteins. *Nucleic Acids Res* 1992; 20: 2603.
- [3] Filippakopoulos P, Picaud S, Mangos M, Keates T, Lambert JP, Barseyte-Lovejoy D, Felletar I, Volkmer R, Müller S, Pawson T, Gingras AC, Arrowsmith CH and Knapp S. Histone recognition and large-scale structural analysis of the human bromodomain family. *Cell* 2012; 149: 214-231.
- [4] Barnett C and Krebs JE. WSTF does it all: a multifunctional protein in transcription, repair, and replication. *Biochem Cell Biol* 2011; 89: 12-23.
- [5] Zanella M, Vitriolo A, Andirko A, Martins PT, Sturm S, O'Rourke T, Laugsch M, Malerba N, Skaros A, Trattaro S, Germain PL, Mihailovic M, Merla G, Rada-Iglesias A, Boeckx C and Testa G. Dosage analysis of the 7q11.23 Williams region identifies BAZ1B as a major human gene patterning the modern human face and underlying self-domestication. *Sci Adv* 2019; 5: eaaw7908.
- [6] Allegri L, Baldan F, Mio C, De Felice M, Amendola E and Damante G. BAZ1B is a candidate gene responsible for hypothyroidism in Williams syndrome. *Eur J Med Genet* 2020; 63: 103894.
- [7] Sun H, Martin JA, Werner CT, Wang ZJ, Damez-Werno DM, Scobie KN, Shao NY, Dias C, Rabkin J, Koo JW, Gancarz AM, Mouzon EA, Neve RL, Shen L, Dietz DM and Nestler EJ. BAZ1B in nucleus accumbens regulates reward-related behaviors in response to distinct emotional stimuli. *J Neurosci* 2016; 36: 3954-3961.
- [8] Ohta S, Taniguchi T, Sato N, Hamada M, Taniguchi H and Rappsilber J. Quantitative proteomics of the mitotic chromosome scaffold reveals the association of BAZ1B with chromosomal axes. *Mol Cell Proteomics* 2019; 18: 169-181.
- [9] Broering TJ, Wang YL, Pandey RN, Hegde RS, Wang SC and Namekawa SH. BAZ1B is dispensable for H2AX phosphorylation on Tyrosine 142 during spermatogenesis. *Biol Open* 2015; 4: 873-884.
- [10] Geiger R, Rieckmann JC, Wolf T, Basso C, Feng Y, Fuhrer T, Kogadeeva M, Picotti P, Meissner F, Mann M, Zamboni N, Sallusto F and Lanzavecchia A. L-arginine modulates t cell metabolism and enhances survival and anti-tumor activity. *Cell* 2016; 167: 829-842, e13.
- [11] Takada I. DGCR14 induces I17a gene expression through the RORγ/BAZ1B/RSKS2 complex. *Mol Cell Biol* 2015; 35: 344-355.
- [12] Mikula M, Rubel T, Karczmarski J, Goryca K, Dadlez M and Ostrowski J. Integrating proteomic and transcriptomic high-throughput surveys for search of new biomarkers of colon tumors. *Funct Integr Genomics* 2011; 11: 215-224.
- [13] Xiao A, Li H, Shechter D, Ahn SH, Fabrizio LA, Erdjument-Bromage H, Ishibe-Murakami S, Wang B, Tempst P, Hofmann K, Patel DJ, Elledge SJ and Allis CD. WSTF regulates the H2A.X DNA damage response via a novel tyrosine kinase activity. *Nature* 2009; 457: 57-62.
- [14] Zhu G, Pei L, Xia H, Tang Q and Bi F. Role of oncogenic KRAS in the prognosis, diagnosis and treatment of colorectal cancer. *Molecular Cancer* 2021; 20: 143.
- [15] Liu Y, Wang SQ, Long YH, Chen S, Li YF and Zhang JH. KRASG12 mutant induces the release of the WSTF/NRG3 complex, and contributes to an oncogenic paracrine signaling pathway. *Oncotarget* 2016; 7: 53153-53164.
- [16] Nagtegaal ID, Odze RD, Klimstra D, Paradis V, Rugge M, Schirmacher P, Washington KM, Carneiro F and Cree IA; WHO Classification of Tumours Editorial Board. The 2019 WHO classification of tumours of the digestive system. *Histopathology* 2020; 76: 182-188.
- [17] Nazet U, Schröder A, Grässel S, Muschter D, Proff P and Kirschneck C. Housekeeping gene validation for RT-qPCR studies on synovial fibroblasts derived from healthy and osteoarthritic patients with focus on mechanical loading. *PLoS One* 2019; 14: e0225790.
- [18] Gong F, Chiu LY, Cox B, Aymard F, Clouaire T, Leung JW, Cammarata M, Perez M, Agarwal P, Brodbelt JS, Legube G and Miller KM. Screen identifies bromodomain protein ZMYND8 in chromatin recognition of transcription-associated DNA damage that promotes homologous recombination. *Genes Dev* 2015; 29: 197-211.
- [19] Cybulska M, Olesinski T, Goryca K, Paczkowska K, Statkiewicz M, Kopczynski M, Grochowska A, Unrug-Bielawska K, Tyl-Bielicka A, Gajewska M, Mroz A, Dabrowska M, Karczmarski J, Paziewska A, Zajac L, Bednarczyk M, Mikula M and Ostrowski J. Challenges in stratifying the molecular variability of patient-derived colon tumor xenografts. *Biomed Res Int* 2018; 2018: 2954208.
- [20] Kopczynski M, Statkiewicz M, Cybulska M, Kuklinska U, Unrug-Bielawska K, Sandowska-Markiewicz Z, Grochowska A, Gajewska M, Ku-

## Oncogenic role of BAZ1B in colorectal cancer

- lecka M, Ostrowski J and Mikula M. Cytotoxic efficacy and resistance mechanism of a TRAIL and VEGFA-peptide fusion protein in colorectal cancer models. *Int J Mol Sci* 2021; 22: 3160.
- [21] Anders S, Pyl PT and Huber W. HTSeq—a Python framework to work with high-throughput sequencing data. *Bioinformatics* 2015; 31: 166-169.
- [22] Love MI, Huber W and Anders S. Moderated estimation of fold change and dispersion for RNA-seq data with DESeq2. *Genome Biol* 2014; 15: 550.
- [23] Yu G, Wang LG, Han Y and He QY. ClusterProfiler: an R package for comparing biological themes among gene clusters. *OMICS* 2012; 16: 284-287.
- [24] Tang Z, Kang B, Li C, Chen T and Zhang Z. GEPIA2: an enhanced web server for large-scale expression profiling and interactive analysis. *Nucleic Acids Res* 2019; 47: W556-W560.
- [25] Shao X, Lv N, Liao J, Long J, Xue R, Ai N, Xu D and Fan X. Copy number variation is highly correlated with differential gene expression: a pan-cancer study. *BMC Medical Genetics* 2019; 20: 175.
- [26] Ahmed D, Eide PW, Eilertsen IA, Danielsen SA, Eknæs M, Hektoen M, Lind GE and Lothe RA. Epigenetic and genetic features of 24 colon cancer cell lines. *Oncogenesis* 2013; 2: e71.
- [27] Dutto I, Tillhon M, Cazzalini O, Stivala LA and Proserpi E. Biology of the cell cycle inhibitor p21 (CDKN1A): molecular mechanisms and relevance in chemical toxicology. *Arch Toxicol* 2015; 89: 155-178.
- [28] Brown DR, Thomas CA and Deb SP. The human oncoprotein MDM2 arrests the cell cycle: elimination of its cell-cycle-inhibitory function induces tumorigenesis. *EMBO J* 1998; 17: 2513-2525.
- [29] Lei K, Bai H, Sun S, Xin C, Li J and Chen Q. PA28 $\gamma$ , an accomplice to malignant cancer. *Front Oncol* 2020; 10: 584778.
- [30] Jiang TX, Ma S, Han X, Luo ZY, Zhu QQ, Chiba T, Xie W, Lin K and Qiu XB. Proteasome activator PA200 maintains stability of histone marks during transcription and aging. *Theranostics* 2021; 11: 1458-1472.
- [31] Sharif SB, Zamani N and Chadwick BP. BAZ1B the protean protein. *Genes* 2021; 12: 1541.
- [32] Uhlén M, Fagerberg L, Hallström BM, Lindskog C, Oksvold P, Mardinoglu A, Sivertsson Å, Kampf C, Sjöstedt E, Asplund A, Olsson I, Edlund K, Lundberg E, Navani S, Szigartyo CA-K, Odeberg J, Djureinovic D, Takanen JO, Hober S, Alm T, Edqvist PH, Berling H, Tegel H, Mulder J, Rockberg J, Nilsson P, Schwenk JM, Hamsten M, von Feilitzen K, Forsberg M, Persson L, Johansson F, Zwahlen M, von Heijne G, Nielsen J and Pontén F. Proteomics. Tissue-based map of the human proteome. *Science* 2015; 347: 1260419.
- [33] Meng J, Zhang XT, Liu XL, Fan L, Li C, Sun Y, Liang XH, Wang JB, Mei QB, Zhang F and Zhang T. WSTF promotes proliferation and invasion of lung cancer cells by inducing EMT via PI3K/Akt and IL-6/STAT3 signaling pathways. *Cell Signal* 2016; 28: 1673-1682.
- [34] Liu Y, Zhang YY, Wang SQ, Li M, Long YH, Li YF, Liu YK, Li YH, Wang YQ, Mi JS, Yu CH, Li DY, Zhang JH and Zhang XJ. WSTF acetylation by MOF promotes WSTF activities and oncogenic functions. *Oncogene* 2020; 39: 5056-5067.
- [35] Yang L, Du C, Chen H and Diao Z. Downregulation of Williams syndrome transcription factor (WSTF) suppresses glioblastoma cell growth and invasion by inhibiting PI3K/AKT signal pathway. *Eur J Histochem* 2021; 65: 3255.
- [36] Jiang D, Ren C, Yang L, Li F, Yang X, Zheng Y, Ji X and Tian Y. Williams syndrome transcription factor promotes proliferation and invasion of cervical cancer cells by regulating PI3K/Akt signaling pathway. *J Obstet Gynaecol Res* 2021; 47: 2433-2441.
- [37] Percipalle P, Fomproix N, Cavellán E, Voit R, Reimer G, Krüger T, Thyberg J, Scheer U, Grummt I and Farrants AK. The chromatin remodelling complex WSTF-SNF2h interacts with nuclear myosin 1 and has a role in RNA polymerase I transcription. *EMBO Rep* 2006; 7: 525-530.
- [38] Barnett C, Yazgan O, Kuo HC, Malakar S, Thomas T, Fitzgerald A, Harbour W, Henry JJ and Krebs JE. Williams syndrome transcription factor is critical for neural crest cell function in *Xenopus laevis*. *Mech Dev* 2012; 129: 324-338.
- [39] Manfredi JJ. The Mdm2-p53 relationship evolves: mdm2 swings both ways as an oncogene and a tumor suppressor. *Genes Dev* 2010; 24: 1580-1589.
- [40] Yang W, Gadgil P, Krishnamurthy VR, Landis M, Mallick P, Patel D, Patel PJ, Reid DL and Sanchez-Felix M. The evolving druggability and developability space: chemically modified new modalities and emerging small molecules. *AAPS J* 2020; 22: 21.
- [41] Chen P, Chaikuad A, Bamborough P, Bantscheff M, Bountra C, Chung C, Fedorov O, Grandi P, Jung D, Lesniak R, Lindon M, Müller S, Philpott M, Prinjha R, Rogers C, Selenski C, Tallant C, Werner T, Willson TM, Knapp S and Drewry DH. Discovery and characterization of GSK2801, a selective chemical probe for the Bromodomains BAZ2A and BAZ2B. *J Med Chem* 2016; 59: 1410-1424.
- [42] Goldman MJ, Craft B, Hastie M, Repečka K, McDade F, Kamath A, Banerjee A, Luo Y, Rogers D, Brooks AN, Zhu J and Haussler D. Visualizing and interpreting cancer genomics data via the Xena platform. *Nat Biotechnol* 2020; 38: 675-678.

**Tumor size vs BAZ1B intensity staining correlation**

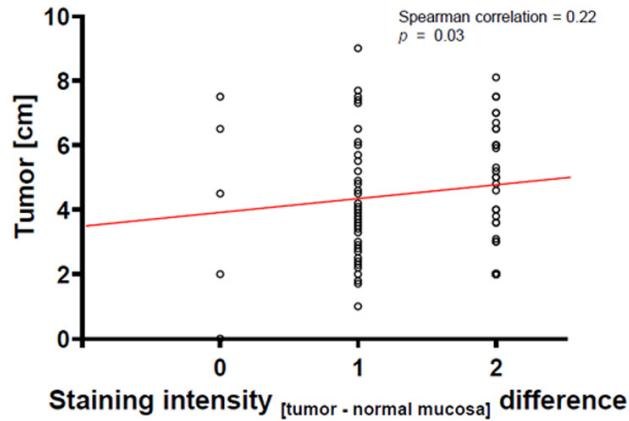


**Figure S1.** Correlation plot of tumor size and BAZ1B intensity staining. Source data are available in [Table S1](#).

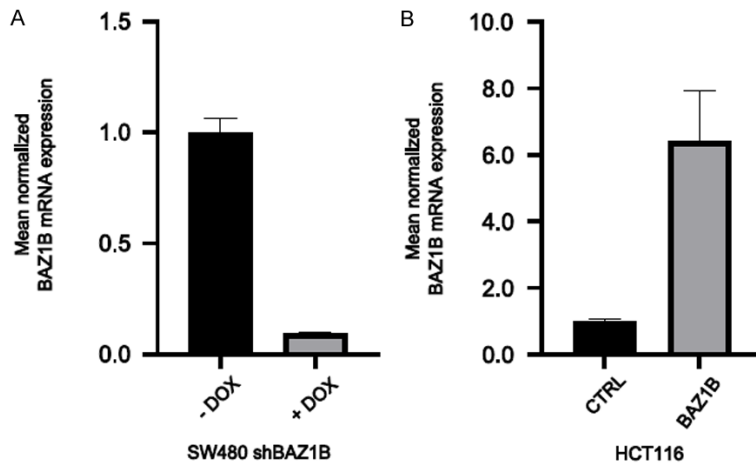


**Figure S2.** BAZ1B mRNA levels in SW480 BAZ1B shRNA (A) and HCT116 BAZ1B (B) transformed cells. RT-qPCR data represent average background-corrected values  $\pm$  SD obtained from three independent experiments.

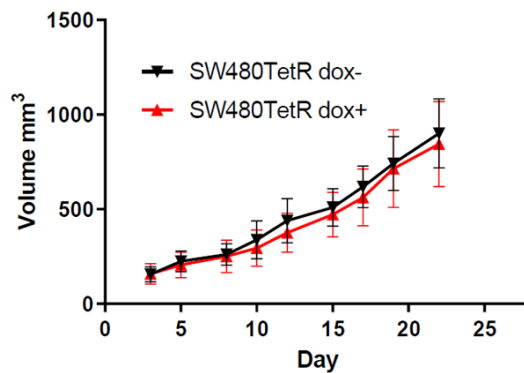


**Figure S3.** Measurements of xenografts derived from SW480 cells encoding only TetR protein (control variant); the graph shows the averaged tumor volumes in subsequent measurements. Doxycycline administration and measurements were initiated when tumors reached an average size of 100 mm<sup>3</sup>, n = 10 for each group, each mouse bearing one tumor,  $\pm$  SD.

## Oncogenic role of BAZ1B in colorectal cancer

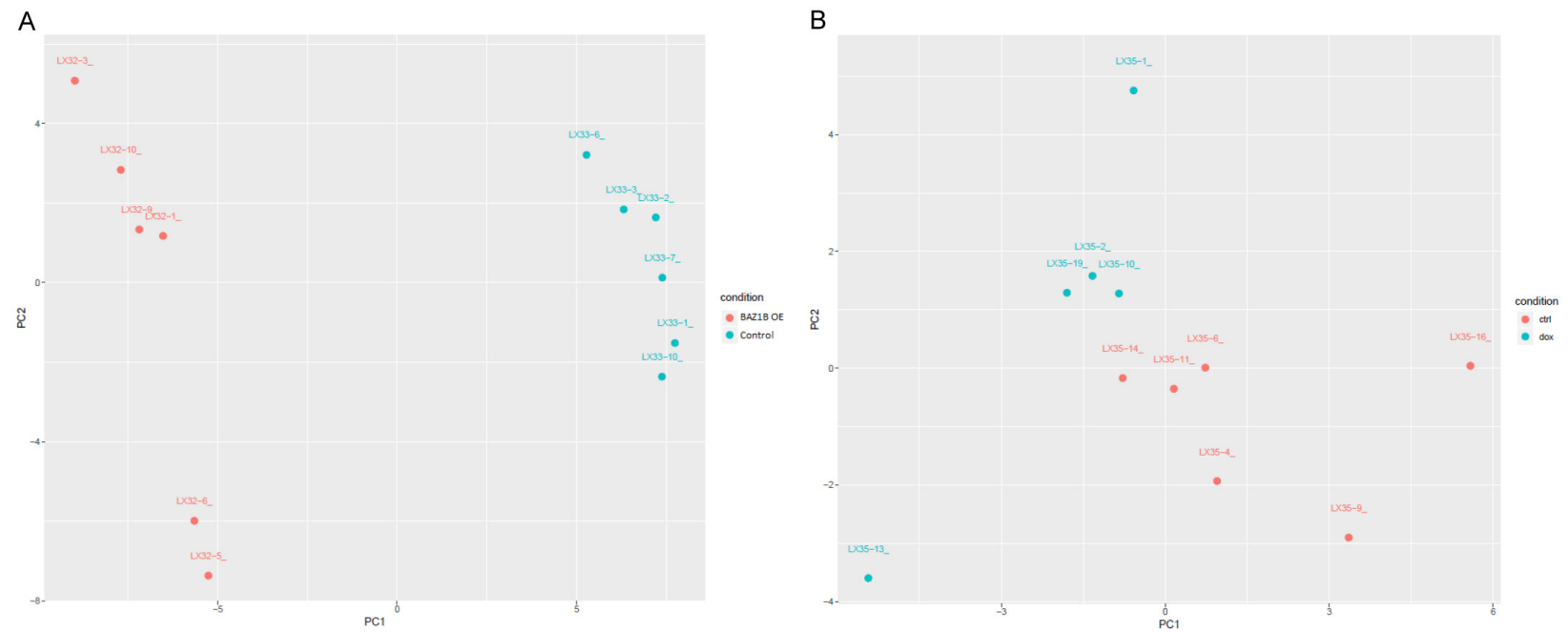


**Figure S4.** Principal component analysis. The first two principal components were computed from transcriptomic data of xenografts established from HCT116 cells with stable BAZ1B overexpression (A) or SW480 cells encoding the BAZ1B silencing system induced by doxycycline (B) as compared to control xenografts. The analysis was performed using the DESeq2 function “plotPCA” with the default parameters.